

Alma Mater Studiorum Università di Bologna  
Archivio istituzionale della ricerca

Is accounting enforcement related to risk-taking in the banking industry?

This is the final peer-reviewed author's accepted manuscript (postprint) of the following publication:

*Published Version:*

Dal Maso L., Kanagaretnam K., Lobo G.J., Mazzi F. (2020). Is accounting enforcement related to risk-taking in the banking industry?. JOURNAL OF FINANCIAL STABILITY, 49, 1-15 [10.1016/j.jfs.2020.100758].

*Availability:*

This version is available at: <https://hdl.handle.net/11585/774470> since: 2023-03-22

*Published:*

DOI: <http://doi.org/10.1016/j.jfs.2020.100758>

*Terms of use:*

Some rights reserved. The terms and conditions for the reuse of this version of the manuscript are specified in the publishing policy. For all terms of use and more information see the publisher's website.

This item was downloaded from IRIS Università di Bologna (<https://cris.unibo.it/>).  
When citing, please refer to the published version.

(Article begins on next page)

This is the final peer-reviewed accepted manuscript of:

Strategies of tailored nanomaterials for electrochemiluminescence signal enhancements

Yemataw Addis Alemu, Enrico Rampazzo, Francesco Paolucci, Luca Prodi and Giovanni Valenti

Current Opinion in Colloid & Interface Science 2022, 61:101621

The final published version is available online at:

<https://doi.org/10.1016/j.cocis.2022.101621>

Terms of use:

Some rights reserved. The terms and conditions for the reuse of this version of the manuscript are specified in the publishing policy. For all terms of use and more information see the publisher's website.

*This item was downloaded from IRIS Università di Bologna (<https://cris.unibo.it/>)*

***When citing, please refer to the published version.***

# Strategies of Tailored Nanomaterials for Electrochemiluminescence signal enhancements

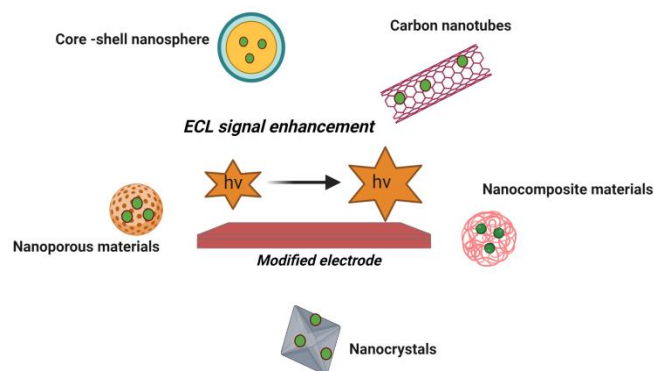
Yemataw Addis Alemu, Enrico Rampazzo, Francesco Paolucci, Luca Prodi,\* Giovanni Valenti\*

*Dipartimento di Chimica “Giacomo Ciamician”, Università degli Studi di Bologna, Via Selmi 2, 40126 Bologna, Italy*

*Corresponding author: Luca Prodi (luca.prodi@unibo.it); Giovanni Valenti (g.valenti@unibo.it)*

**Abstract:** Nanomaterials and their applications were studied extensively over the past few decades due to their properties which are associated mainly with the nanoscale sizes and unique characteristics that they have. Among many applications, these nanomaterials have been playing great, multifaceted roles in increasing the analytical performances of electrochemiluminescence (ECL). In this article, we review the main possible approaches– based on nanoparticles – to modify the photophysical properties of the excited state generated as a consequence of the electrochemical stimulus and in particular taking profit of the so-called metal-enhanced fluorescence (MEF) and resonance energy transfer (RET) processes. We believe that these strategies will lead to the design of very efficient systems that can substantially increase the possible successful applications of ECL.

## Electrochemiluminescence



**Keywords:** Nanomaterials; electrochemiluminescence; localized surface plasmon resonance; resonance energy transfer; biosensors.

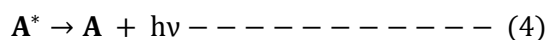
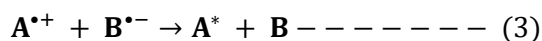
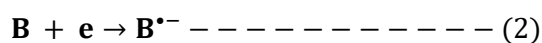
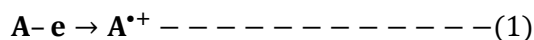
## Abbreviations

ECL, electrochemiluminescence; MEF, metal-enhanced fluorescence; RET, resonance energy transfer; NPs, Nanoparticles; LSPR, localized surface plasmon resonance; SEECCL, surface-enhanced electrochemiluminescence; QDs, Quantum dots; NCs- Nanocrystals; NRs, Nanorods; SPC, Surface plasmon coupled

## 1. Introduction

Electrochemiluminescence (ECL) is the process whereby redox-active species generated at electrode surfaces undergo electron transfer reactions to form excited states that emit light without the need of an external light source [1–4]. The ECL systems are divided – based on the reaction mechanisms and reactants involved – into annihilation ECL and co-reactant ECL. While the early ECL studies were started from annihilation ECL [5], modern ECL systems are almost exclusively of the co-reactant ECL type [6,7]. The annihilation ECL involves the formation of an excited state as a result of electron transfer between two radical ions of the reactants (e.g. A and B) generated at the surface of an electrode applying both positive and negative potentials [8]. This type of ECL system is influenced by the stability of intermediates, their diffusion rate and the voltage windows of solvent.

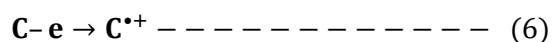
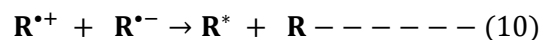
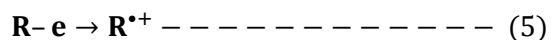
The annihilation ECL is typically based on the following reactions:



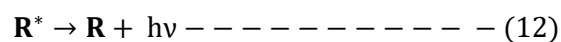
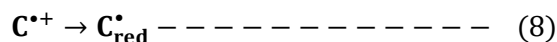
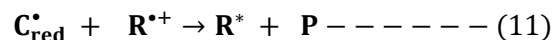
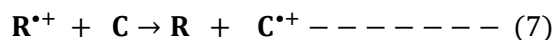
On the other hand, the co-reactant ECL system involves the use of a co-reactant, that produces a strong reducing or oxidizing agent in a reaction following electron transfer by applying a single potential or sweeping the potential in only one direction [9–12]. This system is further classified into “oxidative-reduction” and “reductive-oxidation” pathways.

i) “Oxidative-reduction” co-reactant ECL

$\text{Ru}(\text{bpy})_3^{2+}/(\text{tri-n-propylamine})$  is the most commonly used luminophore/co-reactant pair in this pathway and generally follows three steps: (a) the oxidation reactions on the electrode surface, eq. 5 and 6; (b) bond-breaking or atom-transfer reaction of the co-reactant giving a strong reducing radical, eq. 8; and (c) the reduction of the oxidized luminophore by the co-reactant radical that generates the excited state, eq. 11, that finally emits a photon, eq. 12.



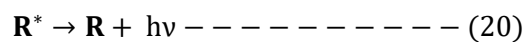
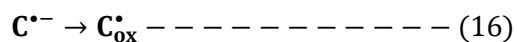
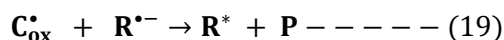
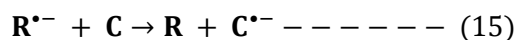
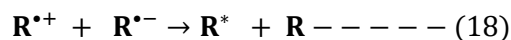
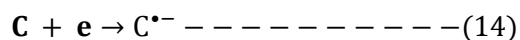
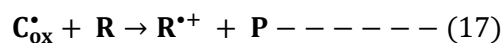
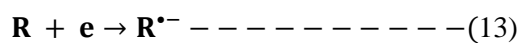
OR



Where R, C,  $C_{\text{red}}$  and P represent the ECL emitter, the co-reactant, the reductive intermediate of the co-reactant, and its product, respectively.

ii) “Reductive-oxidation” co-reactant ECL

For this mechanism to occur, strong oxidants (such as  $\text{H}_2\text{O}_2$  and  $\text{S}_2\text{O}_8^{2-}$ ) are required and both luminophore and co-reactant have to be reduced first. Then, the reduced form of the co-reactant generates a strong oxidizing radical (eq. 16), which further reacts with the reduced luminophore to generate the desired excited state.



Where R, C,  $\text{C}_{\text{ox}}$  and P represent the ECL emitter, the co-reactant, the oxidative intermediate of the co-reactant, and its product, respectively.

ECL is a powerful analytical method that has been widely used in many areas such as immunoassays [13], DNA [14,15], and proteins [9,16,17], analysis, clinical diagnosis,[18], food security [19], environmental monitoring [20], and so forth due to its remarkable advantages, such as wide dynamic range, high sensitivity, low background signal, low cost, good temporal and spatial controllability, simplicity and rapidity [21–25]. For these reasons, ECL is already extensively used in clinical analyses, for example in commercialized immunoassays developed by Roche Diagnostics (Elecsys) and Meso Scale Diagnostics [26]. However, there is still the need to improve the analytical performances to increase the sensitivity even further –to detect the ultra-low concentrations of some biomarkers typical of very early stages of diseases – to increase multiplexing abilities and to extend its possible applications to Point of Care Testing (POCT), an urgent need as also suggested by the problems related to the massive screening required by COVID-19. Therefore, the scientific community has been investing great efforts to develop rapid, reliable and highly sensitive ECL biosensors [27\*\*\*, 28\*\*\*,29\*–32]. To improve the performance of ECL, many researchers have been working on different strategies such as developing various highly luminescent [33], molecules or new reagents [34], efficient co-reactants [35,36], or improving the properties of the electrode surface. In this context, great attention is indeed dedicated to the signal amplification that can be obtained with suitable use of nanotechnology, such as ~~for example~~ encapsulating a large number of luminophores in nanoparticles (such as in  $\text{SiO}_2$  NPs) [26,37], using nanostructured co-reactants [38], and using metal (e.g. Au & Ag) nanostructures to list some of the many strategies [25,27\*\*\*,39-41, 42\*\*–44]. For example, Sojic et al have constructed an ECL system using  $\text{Ru}(\text{bpy})_3^{2+}$  - doped silica /Au nanoparticles (RuDSNs/AuNPs) as ECL nanoemitters for imaging a single biomolecule. With this enhanced ECL system, the group was able to detect cytokeratin 19 (CK19)- a prognostic tumoral and metastatic biomarker with a limit of detection of 0.12 pg/ml [45].

Among the different options, all possibly leading to interesting results, we would like to focus here on the capability, offered by a proper design of NPs, to modify the photophysical properties of the excited state generated as a consequence of the electrochemical stimulus. In particular, we think that two main strategies can emerge in this context. The first one is the possible enhancement of the ECL performance caused by the interaction of plasmons –

typical of metal-based nanostructures – with the luminophores, enabling to increase the luminescence quantum yield (through the so-called metal enhanced effect, MEF) and, thus, the ECL overall emission [17,18,39].

The second strategy is to increase the performances of ECL-based systems taking profit from the occurrence of energy-transfer processes from the excited state generated by the electrochemical reaction – acting as a donor – to a suitably chosen acceptor present in nanostructured systems. It is worth underlining here that this strategy can lead to a signal increase if the luminescence quantum yield of the acceptor is higher than the one of the donor, and to a possible tuning of the emission wavelength, which could lead to an increase of the colours that can be obtained with ECL. In this way, the possibility to perform multiplexing can be easier, a very interesting result since ECL at the moment is mainly based on the orange colour typical of the Ru(II)polypyridine complexes. Since the energy transfer process can occur only at very short distances ( $< 10$  nm), the confinement of both donor and acceptor in nanostructures can be seen as the most promising approach to obtain this effect.

Of course, in both cases, the ECL performance depends also on the size, shape and distance of the nanostructure and its different components [27\*\*\*,29\*]. Therefore, the main aim of this review is to introduce the readers to these two mechanisms – also illustrating some of their applications to biosensors –trying to suggest how to design nanostructures that can efficiently take profit from these approaches, in the belief that this will lead to significant improvements in analytical performances.

## **2. ECL enhancement based on the interaction with localized surface plasmon resonance (LSPR)**

With the advent of nanotechnology, researchers have started to take profit from the interactions of luminophores with metallic surfaces and nanoparticles to design new and, possibly, more sensitive (bio)sensors. In this context, different approaches have been presented for the ECL signal enhancements through metal NPs and their nanocomposites [46]. One possible strategy is the design of a nanostructured electrode endowed with an increased surface area, boosting in this way the electron transfer between the electrode and ECL reactants [47–49]. Here we will focus more on the photophysical changes induced by the presence of the metallic nanostructures in an approach based on the localized surface plasmon resonance (LSPR).

The complete description of the theory that is behind the interaction between a luminophore and a metal (nano)structure, which can lead to both luminescence quenching or enhancement, is outside the scope of this article, and we invite the interested readers to more specialized reviews, starting from the pioneering work of Lakowicz [50]. In particular, Lakowicz introduced the concept of radiating plasmons (RPs). According to this approach, the formation of the excited state of the luminophore induces a charge redistribution on the metal surface: if this plasmon can radiate, then the luminophore emission is observed as plasmon-coupled emission, *i.e.*, having the spectral characteristics of the luminophore; otherwise, the luminescence is quenched [50]. Despite the large enhancements that could be obtained, limited examples of practical and effective studies are reported, at present times, where the great enhancing plasmon potentials are fully merged with chemiluminescence and ECL sensors [50]. The reason for that may be not the trivial balance between emission enhancing and quenching, due to the interaction with the metal surfaces, mostly depending on the distance at which the luminophore is placed in respect

of the metal surface. For metallic NPs, Lakowicz suggested to separate their plasmon resonance bands in their scattering and absorption components, indicating that an enhancement of the luminescence can be observed when, at the emission wavelength of the dye, scattering prevails against absorption; otherwise quenching has to be expected. The ratio between these two components depends on the metal used to synthesise the colloid, on its dimension and on its shape. On the basis of this discussion, Lakowicz indicated 40 nm as the optimal size for having metal-enhanced fluorescence (MEF). It is also to note that, for example in gold nanorods, the two components can prevail in different spectral ranges, so that with the same colloid, a dye can be quenched and another one, emitting in a more suitable region, can undergo luminescence enhancement. A limitation of the theory based on the RPs is that it does not take into account of other possible mechanisms, and in particular electron transfer processes, able to quench, typically at very short distances, the luminescence of the dye. However, this theory can give interesting suggestions, and agrees, for example, with the sharp angular distribution into the underlying glass substrate of the ECL emission of Ru(bpy)<sub>3</sub><sup>2+</sup> on a gold film [50,51].

More recently, other authors, including Polo and co-workers, have investigated the effect of SPR of gold film on ECL signal intensity of Ru(bpy)<sub>3</sub><sup>2+</sup>. The group was able to get a 1.7-fold ECL signal enhancement compared to that of without the gold film, and also observed a quenching effect within a 10 nm distance between the luminophore and the gold film [52]. The groups of Guo and Lin [53], discussed the surface-enhanced ECL emission, in particular of Ru(bpy)<sub>3</sub><sup>2+</sup>. As also Lakowicz suggested, they indicated that the surface plasmons of noble metal NPs are excited by the excited state of the ECL luminophores produced on the surface of the electrode, forming evanescent electromagnetic fields around the metal surface (for example see in **Fig.1**). According to these authors, these electromagnetic fields increase the excitation rate and ECL quantum yield of the luminophores which is a measure of ECL efficiency (see eq. 21, described by Wang and co-workers [53]) and such kind of ECL is named surface-enhanced ECL (SEECL) [1,18,28\*\*\*,53].

$$\text{MDE}(\mathbf{r}_o) = \underbrace{\Gamma_{\text{exc}}(\mathbf{r}_o)}_{\text{Excitation}} * Q * \underbrace{\text{MCE}(\mathbf{r}_o)}_{\text{Emission}} \text{-----} (21)$$

Where  $\Gamma_{\text{exc}}(\mathbf{r}_o)$  is the excitation rate,  $Q$  is the ECL quantum yield,  $\text{MCE}(\mathbf{r}_o)$  is the molecular collection efficiency function at point  $\mathbf{r}_o$  ( $Q \times \text{MCE}(\mathbf{r}_o)$  is an emission factor).

SEECL signal intensity depends on different factors, the first one being the degree of overlapping between the ECL emission spectra of luminophores and the UV-Vis absorption spectra of LSPR of metals. The ECL emission light of the luminophores that interacts with the surface of the metal nanostructures has to be similar with that of LSPR band as much as possible to generate LSPR-field which in turn affects the enhancement of ECL. Therefore, when there is a good overlapping between the ECL emission of luminophore and the LSPR band of the metal nanostructures, an enhanced ECL signal can be obtained [39,54].

The second important factor is the distance between ECL emitters and plasmonic material: the inter-distance between the metal nanostructures and the ECL emitter can be fixed by using linkers of controlled length

such as DNA or by controlling the thickness of the shell (for example, an outer SiO<sub>2</sub> shell) and it is a very important factor for LSPR based ECL enhancement. It should be noted however that there is always a competition between LSPR-field enhancement of ECL and ECL quenching, due to energy or electron transfer processes between metal nanostructure and the luminophore. If the nanostructure and the luminophore are very close to each other, the quenching effect typically dominates. On the other hand, the LSPR-field based ECL enhancement dominates at higher distances, typically longer than 10 nm. However, further increasing the separation distance will result in a decrease in the ECL intensity because of a decrease in LSPR electromagnetic field. Therefore, optimized separation distance is always required [39,53].

A third factor is the size and shape of the nanostructure: -their changes affect the ECL intensity due to different aspects. For example, different sizes and shapes of the metal nanostructures have different nanostructured surfaces which determine the degree of interaction with the nearby excited luminophores. Therefore, appropriate sizes (preferably smaller sizes) with shapes of the metal nanostructures are required to obtain significantly enhanced ECL signals [54–56\*].

Finally, another important element to be considered is the nature (type) of the plasmonic material. The level of LSPR-based ECL intensity enhancement strictly depends on the type of metal nanostructures mainly because this confers different optical and electrochemical properties. For example, Li and co-workers have found that the ECL intensity of gold NPs has shown a great enhancement compared to that of Ag NPs and Pt NPs in the determination of diclofenac [57,58].

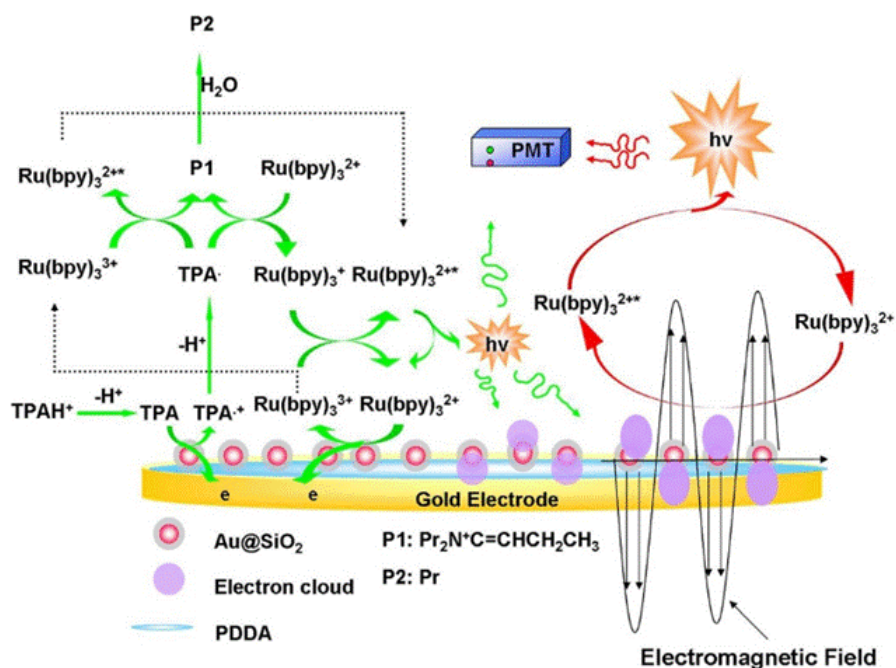


**Fig. 1** The schematic diagram of SEECL. The figure is adapted from ref. [53]

Many researchers have developed different LSPR-based SEECL biosensors for the analysis of various analytes and biomarkers. For instance, Li and co-workers have designed Au@SiO<sub>2</sub>-NH<sub>2</sub>/CdS/GCE ECL biosensor for the detection of glutathione (a biomarker for many diseases such as diabetes, liver, Alzheimer, and Parkinson)



and they have found about 35-fold enhanced ECL signal compared to the same electrode but in the absence of Au. The separation distance of Au NPs and CdS QDs was controlled by the thickness of silica shells [1]. Ma *et al.* have fabricated an Au–Au NP dimer-based surface plasmon coupling ECL (SPC-ECL) sensor for the detection of breast cancer susceptibility gene 1 (BRCA1 genes). The ECL emitter was graphite phase carbon nitride (g-C<sub>3</sub>N<sub>4</sub>) QDs (GCN QDs). Carbon nitride is a two-dimensional nanomaterial that is composed of a large number of carbon and nitrogen elements and has an attractive electronic structure, optical properties, and shows various functions such as in fluorescent probes [59]. In this case, the gap distance between the two Au NPs was controlled by the length of DNA that was used as a connector to form the dimers. The DNA chain was used not only to regulate the distance but also to keep the binding site for biosensing. Due to the hot spot effect (responsible for the high electromagnetic field distributed around the dimer) at the junction of the two Au NPs, the electrode modified with Au–Au dimers enhanced the ECL signal of GCN QDs compared to that of electrodes without the dimers [57]. In another example, Lin's group has constructed SEECL signal of Ru(bpy)<sub>3</sub><sup>2+</sup> for the ultrasensitive detection of prostate-specific antigen (PSA) in human serum based on LSPR using Au coated by silica. The ECL signals of modified gold electrodes with and without Au were compared and the ones in the presence of Au have shown a stronger ECL signal, attributed to the LSPR of Au [27\*\*\*].

Furthermore, Wang *et al.* have prepared a LSPR-based SEECL ultrasensitive sensor for the detection of Hg<sup>2+</sup> using Ru(bpy)<sub>3</sub><sup>2+</sup> as ECL emitter and gold nanorods (AuNRs) as a source of LSPR. The distance between Ru(bpy)<sub>3</sub><sup>2+</sup> and AuNRs was controlled by using spacers of DNA and the effect on the intensity of the ECL signal was well demonstrated. Moreover, the overlapping of the absorption spectrum of LSPR of AuNR (according to Lakowicz [50], to its scattering component) and the ECL emission spectrum of Ru(bpy)<sub>3</sub><sup>2+</sup> was observed which is one of the requirements for ECL signal enhancement due to LSPR [39]. Cao *et al.* have developed Au@SiO<sub>2</sub>@RuDS/GCE nanocomposite-based plasmon-enhanced ECL sensor (RuDS; Ru(bpy)<sub>3</sub><sup>2+</sup>-doped silica) for the highly sensitive detection of glutathione (GSH) [21]. The intensity of Au@SiO<sub>2</sub>@RuDS/GCE ECL biosensor was compared with that of other differently modified GCEs. As can be observed from **Fig. 2A**, the ECL intensity of Au@RuDS/GCE is lower than that of RuDS/GCE, because of the quenching effect of AuNPs on the ECL signal of Ru(bpy)<sub>3</sub><sup>2+</sup> through electron/energy transfer. On the other hand, the ECL intensity of Au@SiO<sub>2</sub>@RuDS/GCE is 2.3 times higher than that of RuDS/GCE because of the LSPR effect of AuNPs. The thickness of the silica shell was used to control the separation distance between Au NPs and Ru(bpy)<sub>3</sub><sup>2+</sup>. As is mentioned in the first paragraph of section 2, there is always a quenching at closer distance (because of electron/energy transfer) and LSPR enhancing competition effects ECL intensity. However, when they further increased the thickness of silica (> 13 nm), and thus the separation distance between Au NPs and Ru(bpy)<sub>3</sub><sup>2+</sup>, they found a reduced ECL signal due to a decline of LSPR electromagnetic field effect [21].

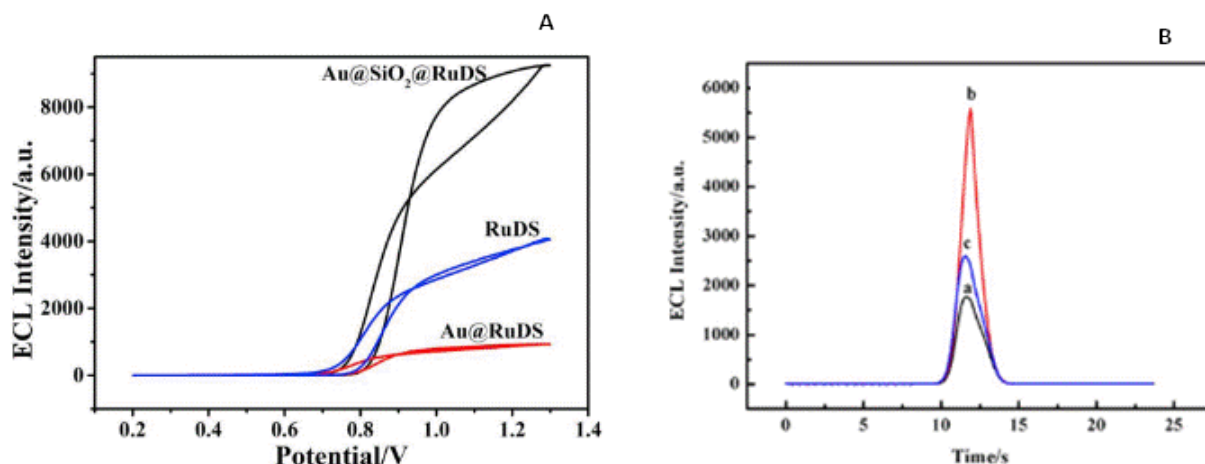


**Fig. 2** A) ECL curves of Au@RuDS/GCE, RuDS/GCE, and Au@SiO<sub>2</sub>@RuDS/GCE in 0.10 M PBS (pH 7.5) containing 10 mM TP B) ECL responses of (a) MIP/Ru@SiO<sub>2</sub>/CS/GCE, (b) MIP/Ru@SiO<sub>2</sub>/CS/AuNPs/GCE and (c) Ru@SiO<sub>2</sub>/CS/MIP/AuNPs/GCE in 0.1 M PBS (pH = 7.0). **Fig. 2A and 2B** are adapted from ref. [21] and [9] respectively, with permissions from Elsevier.

Wang's group has also prepared a SEECCL for ultrasensitive detection of carcinoembryonic antigen (CEA, a biomarker for various cancers) using two aptamers to sandwich CEA, AuNPs as a source of LSPR, and Ru@SiO<sub>2</sub> as luminophores. They showed a 30-fold enhanced ECL signal from the modified gold electrode in the presence of AuNPs compared to the ECL signal obtained without the gold nanostructures [18]. Kitteet *et al.* have developed a sensitive aptamer-based, sandwich-type surface plasmon-enhanced ECL(SPEECL) immunosensor for the detection of cardiac troponinI (cTnI, the most used biomarker for the diagnosis of acute myocardial infarction), using aptamer conjugated CdS QDs and AuNPs as ECL luminophores and plasmon sources, respectively. The signal of the developed SPEECL system showed about a 5-fold increment compared to the one obtained without AuNPs. The optimum separation distance between CdS QDs and AuNPs was controlled by the length of the aptamers; *i.e.*, by varying the numbers of thymine (T) in the capture-probe pair. The maximum ECL intensity was found when the number of 'T' was 15 in both aptamers. In addition, they have evaluated the degree of overlapping of CdS QDs ECL emission spectrum and the Au NPs UV-Vis absorption spectrum to confirm if the ECL signal enhancement is due to LSPR [29\*].

The Zhao's group designed an enzyme-assisted ultrasensitive ECL biosensor – based on the enhanced signal of CdS nanocrystals due to their interaction with the LSPR of AuNPs dimers – for the detection of microRNA-21, which plays a crucial role in many biological functions and diseases including development, cancer, cardiovascular diseases, and inflammation [60]. The ECL intensities of different modified GCE electrodes were compared; the one with AuNP dimers showed a 6.3-fold enhancement due to LSPR [61]. Zhang *et al.* have fabricated a surface-enhanced molecularly imprinted ECL (MIP/Ru@SiO<sub>2</sub>/CS/AuNPs/GCE) biosensor based on LSPR for the ultrasensitive detection of fumonisin B1, a toxic and cancerogenic mycotoxins found mainly in maize. This group has compared the ECL response of three different modified electrodes to know the mechanism or source of ECL signal enhancement. As shown in **Fig. 2B**, the ECL intensity of the MIP/Ru@SiO<sub>2</sub>/CS/AuNPs/GCE modified

electrode (curve b) was much stronger than the one without AuNPs (curve a), and the ECL enhancement was attributed to the LSPR of AuNPs. On the other hand, the ECL signal of Ru@SiO<sub>2</sub>/CS/MIP/AuNPs/GCE (curve c) modified electrode was less intense than that of MIP/Ru@SiO<sub>2</sub>/CS/AuNPs/GCE because of the higher separation distance between the Ru(bpy)<sub>3</sub><sup>2+</sup> NPs and AuNPs, causing a lower surface plasmon enhanced ECL [9]. By coating ITO electrode with Au@SiO<sub>2</sub>, Li's group was able to find over 1,000 times ECL intensity for Ru(bpy)<sub>3</sub><sup>2+</sup>/TPrA system compared to the bare ITO electrode due to LSPR, making the detection of the prostate-specific antigen (PSA) possible with the remarkable detection limit of 3 fg [62].

During the design of the SEECL biosensors, the researchers usually perform electrochemical impedance spectroscopy (EIS) experiments (for example as shown in Nyquist plots in **Fig. 3A**) to analyse the changes in the electron transfer resistance ( $R_{et}$ ) [9,18]. The semicircle diameter obtained from the Nyquist plots of EIS represents the interfacial resistance at the electrode surface. The higher the semicircle diameter indicates a greater  $R_{et}$  value [27\*\*\*].

As we have already discussed, evaluating the effects of the separation distances between ECL emitters and noble metals (sources of LSPR) on the ECL intensity is a common practice to see whether LSPR is responsible for the observed enhancement, and so is the examination of the overlap between the ECL emission spectrum of the emitter and absorption spectrum of LSPR of metals (**Fig. 3B**) [61,62].

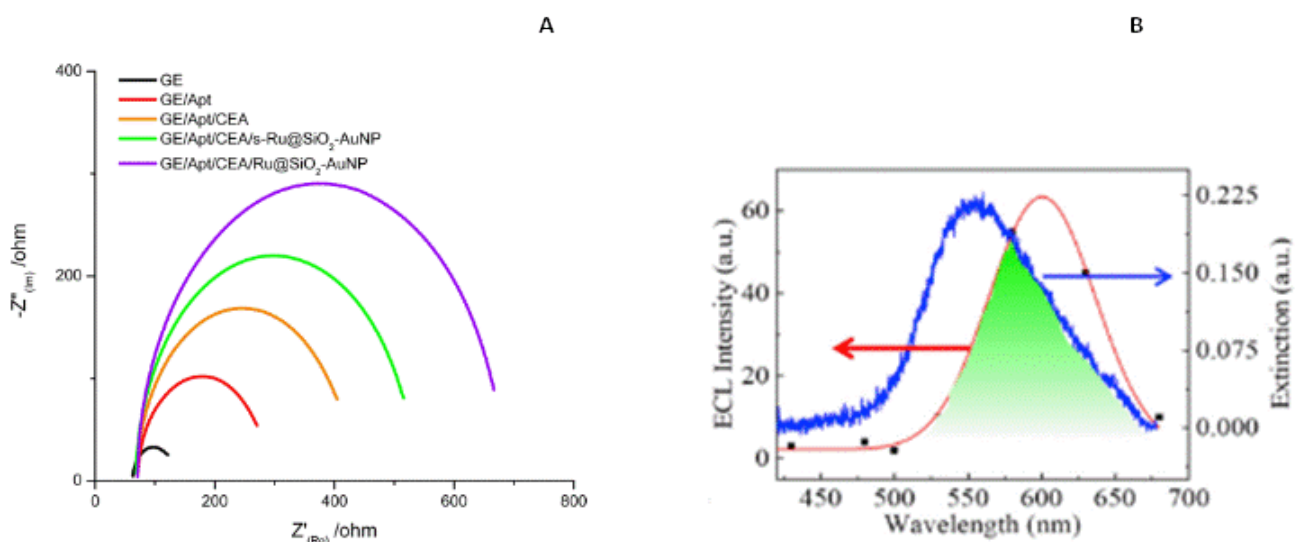


**Fig. 3 A)** Nyquist plots of different modified electrodes. The Nyquist plots were recorded in PBS solution (0.1 M, pH = 7.0) containing 5.0 mM K<sub>3</sub>Fe(CN)<sub>6</sub> with the biasing potential 0.21 V and 5 mV alternative voltage in the frequency range of 1–100000 Hz . **Fig. 3A** is adapted from ref. [18] with a permission from American Chemical Society **B)** Spectra overlap between the emission spectrum of Ru(bpy)<sub>3</sub><sup>2+</sup> and extinction spectrum of Au@SiO<sub>2</sub>. **Fig. 3B** is adapted from ref. [62] with a permission from Elsevier.

However, confirmatory experiments which prove the absence of contributions of other factors such as catalytic activity and electrochemical effects (surface area and electron transfer, etc.) should also be performed since the ECL enhancement effects due to these terms can be significant. For instance, Zhao's group has explored electrochemical measurements of three different modified electrodes by cyclic voltammetry (CV) in 0.1 M PBS (pH 7.0). As shown in **Fig. 4**, no redox peaks have been observed in the selected potential window after dropping AuNPs on the electrode (curve a). However, a pair of redox peaks can be obtained when the electrode was coated only with Ru@SiO<sub>2</sub>/Chitosan (curve b), and the peak current increased markedly after the following introduction of AuNPs (curve c). Based on these results, the group has confirmed that there was a contribution to the enhanced ECL signal by the electrochemical effect due to the increase of the electrode surface area after modification of the electrode by AuNPs. The conclusion after evaluating all data has been that both the LSPR and electrochemical effect of AuNPs contributed to the enhancement of ECL intensity [9].

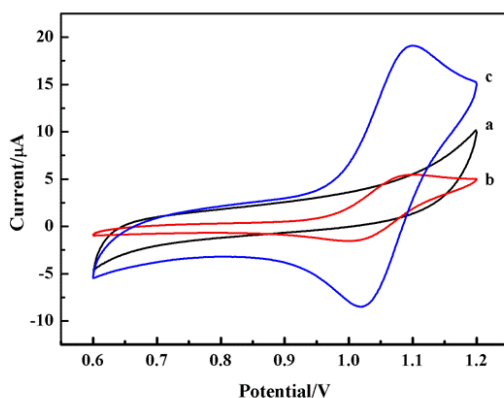


**Fig. 4** CV curves of (a) AuNPs/GCE, (b) Ru@SiO<sub>2</sub>/Chitosan/GCE and (c) Ru@SiO<sub>2</sub>/Chitosan/AuNPs/GCE in 0.1 M PBS (pH 7.0). The figure is adapted from ref. [9] with a permission from Elsevier.

### 3. Resonance energy transfer ECL (ECL-RET)

As we have already mentioned, an improvement in the performances of biosensors can be obtained by exploiting ECL-RET processes, *i.e.*, through an efficient energy transfer between the donor generated in the electrochemical process and a suitable acceptor. ECL with multicolour and tuneable intensities can also be obtained by resonance energy transfer (RET), a feature that is crucial for multiplexed bioassays and analysis [63]. For example, our group has developed – to take profit of this effect – different core-shell silica-PEG NPs containing different combinations of 9,10-diphenylanthracene (**DPA**), a cyanine 5(**C**) and rhodamine B (**RhB**); in particular **DPA** and **C** could be confined on the shell, while **RhB** in the silica core. **DPA**@NPs were able to give in water a blue ECL signal with maximum at ca 430 nm, very similar to the one showed by only **DPA** in aprotic media, while **RhB**@NPs showed an ECL emission at 570 nm. It is important to note here that free **RhB**, not included in NPs, is unable to give ECL emission, because of electrode passivation. In NPs containing both **DPA** and **RhB**, the only signal obtained has been the one at 570 nm, because of the highly efficient energy transfer achievable in this kind of nanoarchitectures [64]. When also **C** was present inside the NPs in combination with **DPA** and/or **RhB**, it was

possible to observe only its emission at 670 nm, indicating again that the energy could be funnelled to the lowest energy acceptor. In this way, three different colours could be obtained with simple chemical modifications, also increasing the possible molecules that could participate in the generation of the final signal [4].

In another example, Ru(II) complexes have been used as energy acceptors in combination with CdS QDs [65], g-C<sub>3</sub>N<sub>4</sub> nanosheet [66], and luminal [67]; interestingly, the same complexes could act as donors if they are close to acceptors such as CdTe QDs having higher quantum yields. Chen and co-workers have developed an ECL-RET sensor by co-encapsulating the donor ([Ru(bpy)<sub>3</sub>]<sup>2+</sup>) and acceptor (CdTe QDs) into a single silica nanosphere eliminating the effect of separation distance and thus obtaining an enhanced ECL performance for the detection of mycotoxins ( $\alpha$ -ergocryptine and ochratoxin A). The authors have also demonstrated that there was a good overlapping between the emission band of the donor and the absorption of the acceptor (**Fig. 5A**), a required feature to an ECL-RET process from Ru(bpy)<sub>3</sub><sup>2+</sup> to CdTe QDs [68].

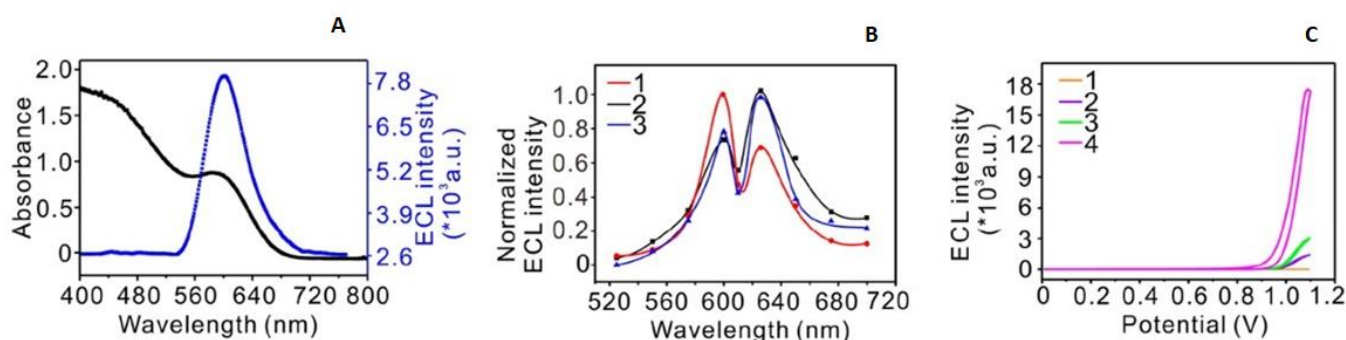


**Fig. 5** **A)** UV–Vis absorption spectrum of CdTe QDs (black) and ECL spectrum (blue) of Ru@SiO<sub>2</sub>/GCE **B)** Normalized ECL spectra of CdTe-Ru@SiO<sub>2</sub>/GCE with different ratio of Ru(II) to CdTe, here the content of Ru(bpy)<sub>3</sub><sup>2+</sup> was fixed at 170 µl (80 mM) and CdTe QDs with different amounts (curve 1, 30 µl; curve 2, 170 µl; curve 3, 310 µl) were used; **C)** ECL responses of CdTe@SiO<sub>2</sub>/GCE (curve 1), Ru@SiO<sub>2</sub>/GCE (curve 2), Ru@SiO<sub>2</sub>/GCE with 5 µl CdTe in solution (curve 3), and CdTe-Ru@SiO<sub>2</sub>/GCE (curve 4) . The figure is adapted from ref. [68] with a permission from American Chemical Society.

Furthermore, the ECL spectra of CdTe-Ru@SiO<sub>2</sub>/GCE with a different ratio of Ru(II) to CdTe inside the nanospheres were compared. As it can be seen in **Fig. 5B**, the ECL-RET leads to a decrease of the ECL emission of Ru(bpy)<sub>3</sub><sup>2+</sup> centred at 599 nm upon the increase of the amount of CdTe QDs, with a concomitant significant increase of the CdTe QDs emission at 627 nm. In addition, the ECL intensity of different modified electrodes has been compared (**Fig. 5C**), and the intensity obtained from CdTe-Ru@SiO<sub>2</sub>/GCE is the one showing the highest enhancement. All these results have proved the existence of an efficient energy transfer process from Ru(bpy)<sub>3</sub><sup>2+</sup> to the CdTe QDs [68].

Li *et al.* have also designed ECL-RET system within one nanostructure containing tris(4,4'-dicarboxylicacid-2,2'-bipyridyl) Ru(II) dichloride (Ru(dcbpy)<sub>3</sub><sup>2+</sup>) as an energy donor and CdSe@ZnS QDs as acceptor. The ECL intensity of the QDs-Ru(dcbpy)<sub>3</sub><sup>2+</sup> composite was higher compared to the ECL intensity of QDs and used to detect miRNA-141, a relevant biomarker for human prostate cancer cells. The ECL emission spectra of

$\text{Ru(dcbpy)}_3^{2+}$  and UV-Vis absorption spectra of QDs have shown a significant overlap, supporting the possibility of occurrence of ECL-RET from  $\text{Ru(dcbpy)}_3^{2+}$  to QDs [69].

Xu's group has designed different ECL-RET systems for the detection of various analytes and biomarkers. For example, they have fabricated an ECL-RET from Mn-doped-CdS NCs ( $\text{Mn@CdS}$ ) to Au NPs for the detection of DNA. The distance between CdS:Mn NCs and AuNPs was regulated by the length of a DNA hairpin [70]. They have also developed an ECL-RET system from CdS QD as a donor and  $\text{Ru(bpy)}_3^{2+}$  as an acceptor for sensitive cytosensing [71].

Xu's group has designed a gold NP-enhanced ECL-RET system from CdS NC thin film as ECL emitter and Au NPs to determine thrombin. Their designed system showed a 5-fold enhancement of ECL signal as compared to that without Au NPs due – according to their justification – to an energy transfer from the excited AuNPs to the CdS NCs [24]. To have more insight into the mechanism responsible for the ECL emission of their system, they performed control tests without Au NPs and CV experiments. Overall, the results showed that Au NPs could increase the effective surface area of the electrode and enhance the rate of electron transfer, as also shown by the current peaks in the CV experiments, demonstrating a synergistic combination with the energy transfer process [22].

Xu's group has tried to prove the occurrence of RET as a possible mechanism for the ECL enhancement. In particular, they did a control experiment with and without the involvement of AuNPs. They have also checked the overlapping of the ECL emission spectra (energy donors) with that of UV-Vis absorption spectra of the energy acceptors. The trend of ECL emission intensity peaks of energy acceptors and donors was evaluated by varying the concentration ratios of the two. As the concentration of  $\text{Ru(bpy)}_3^{2+}$  increased, its ECL emission intensity peak (at 620 nm) increased, a result that has been taken as the confirmation of the occurrence of ECL-RET from CdS (donor) to  $\text{Ru(bpy)}_3^{2+}$  (acceptor) [24,70,71]. Dong et al have designed an ECL-RET-based aptasensor between luminol as an ECL donor and CdSe@ ZnS QDs as an acceptor, which was used for sensitive detection of thrombin [72].

Moreover, Zhang and co-workers have developed an enhanced ECL-RET system for the detection of an ovarian cancer biomarker called lipolysis stimulated lipoprotein receptor (LSR). In their system,  $\text{Ru(bpy)}_3^{2+}$  acted as a donor and CdZnSe@ZnSe QDs as the acceptor of ECL-RET.  $\text{TiO}_2$  metal-organic frameworks ( $\text{TiO}_2$  MOFs) were used for loading  $\text{Ru(bpy)}_3^{2+}$  and the complex with numerous horseradish peroxidases (HRPs) to immobilize CdZnSe@ZnSe QDs. To prove the occurrence of effective ECL-RET, the group has done some confirming experiments. First, as can be seen in **Fig. 6A**, there was a good overlap of the UV-Vis absorption spectrum ( $\lambda_{\text{max}} = 620\text{nm}$ ) of CdZnSe@ZnSe QDs and the ECL emission spectrum ( $\lambda_{\text{max}} = 617\text{ nm}$ ) of  $\text{Ru(bpy)}_3^{2+}$  [73\*\*].



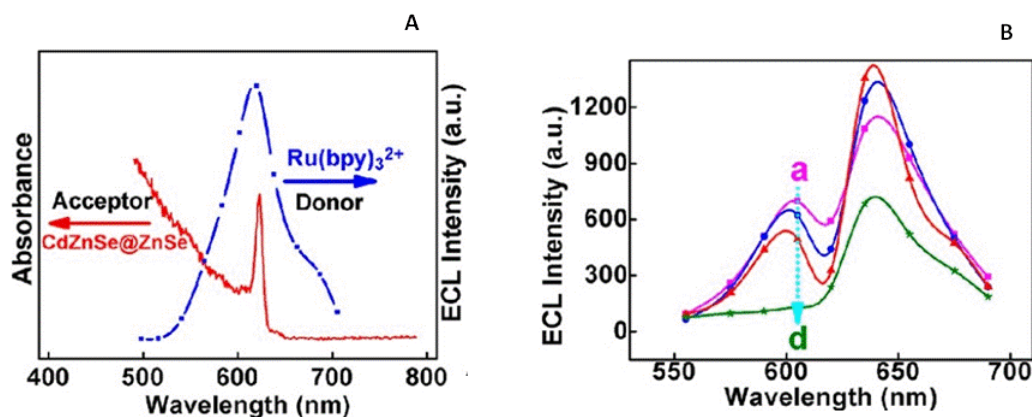


**Fig. 6** **A)** UV–Vis absorption spectrum of CdZnSe@ZnSe QDs (red line) and ECL emission spectrum of Ru(bpy)<sub>3</sub><sup>2+</sup> (blue line). **B)** UV–Vis absorption spectrum of CdZnSe@ZnSe QDs (red line) and ECL spectrum of Ru(bpy)<sub>3</sub><sup>2+</sup> (blue line). The figure is adapted from ref. [73\*\*] with a permission from American Chemical Society.

Further support to the occurrence of the energy transfer process came from observing the intensity of the ECL signals at different concentration ratios of Ru(bpy)<sub>3</sub><sup>2+</sup> and CdZnSe@ZnSe QDs. As the concentration of CdZnSe@ZnSe QDs increased, they were able to observe a decrease of the ECL emission attributable to Ru(bpy)<sub>3</sub><sup>2+</sup> and a concomitant remarkable increase at 635 nm, attributable to the luminescence of CdZnSe@ZnSe QDs (**Fig. 6B**), in line with the occurrence of ECL-RET [73\*\*].

Lu *et al.* have designed ECL-RET system using Ru(bpy)<sub>3</sub><sup>2+</sup>-doped silica NPs (RuSi NPs) as the ECL donor and hollow Au nanocages as the ECL acceptor for detection of miRNA141 and the separation distance was regulated by Tetrahedron DNA (a three-dimensional DNA nanostructure which has many applications in the construction of biosensors) [74,75]. The ECL-RET system based on the electronic excitation energy transfers from GO–Au/RuSi@Ru(bpy)<sub>3</sub><sup>2+</sup>/Chitosan composites as ECL donor and Au@Ag<sub>2</sub>S NPs ECL acceptor for specific detection of target DNA was constructed by Wu and co-workers. The distance was controlled by the length of DNA. Compared to RuSi@Ru(bpy)<sub>3</sub><sup>2+</sup>/Chitosan, the ECL signal observed by the application of GO–Au/RuSi@Ru(bpy)<sub>3</sub><sup>2+</sup>/Chitosan composites was enhanced by 5-fold [25]. Wang’s group has designed an ECL-RET/surface plasmon coupled ECL (SPC-ECL) nanosensor for the detection of Shiga toxin-producing *Escherichia coli* based on boron nitride (BN) QDs as luminophores and Au causes of RET and SPC. The distance between BN QDs and Au NPs was controlled by hairpin DNA [2].

#### 4. Conclusion

Among many possible mechanisms, LSPR and RET can have great effects on the enhancement of the ECL signal intensities and can thus be used in the design of ultrasensitive biosensors for the detection of various analytes of biomedical and environmental interest.

In the case of LSPR-ECL system, the theory behind this effect is complicated and other effects— such as electron transfer processes – can occur, making the overall interpretation difficult. We have however gathered from

previous literature possible strategies to design nanostructured architectures – in particular, their material, their size, their shape and their optical properties, that can benefit from this effect, that in some cases has led to impressive enhancements. We recommend, in all cases, to make a proper characterization of the systems to disentangle all possible contributions to the final ECL signal, both leading to its decrease or enhancement. This is frequently not a simple task, since the rigorous quantification of the single factors influencing the brightness of a LSPR-ECL system requires the comparison with corresponding reference systems in which contributions such as the LSPR and electron-transfer processes involving the metal surface are excluded. In the case of metal@SiO<sub>2</sub> nanostructures, for example, reference counterparts can be obtained by removing the metal from the initial system, to preserve all the other features that need to be evidenced during the characterization. Chemical modifications like this need to be optimized and carefully evaluated since they may influence the starting colloidal properties of the systems that are under investigation.

Large enhancements of the emitted light can be the result of a properly designed ECL-RET system. In this case the theory behind the process is more largely understood but, again, concomitant processes can occur. Interestingly, in this case, the nanostructure can play the role of the energy- donor or acceptor, or as a scaffold to keep the donor-acceptor couple (in this case typically represented by molecular dyes) at the proper distance to make the process efficient. Also in this case, the types and occurrences of these ECL enhancement mechanisms have to be supported by experimental pieces of evidence, such as a suitable overlap between the ECL emission spectrum of the ECL emitter and the absorption spectra of the final acceptor. Investigating the effect of the separation distance (for example the thickness of a silica shell and the length of a DNA sequence) between the donor-acceptor couple is also another confirmatory experiment. Using different concentration ratios of the ECL-RET donor and acceptors in the nanostructures (nanocomposites) is also very important evidence to confirm that the mechanism of ECL enhancement is due to RET. It is important to underline that, with this approach, it is possible not only to increase the final intensity of the ECL emission but also to tune its wavelength, paving the way for a more flexible approach to multiplexing, a point of weakness, so far, of the ECL technology.

**Acknowledgments:** Financial support from the University of Bologna and from the Italian Ministry of University and Research (MUR), Project PRIN 2020CBEYHC, is gratefully acknowledged.

## References

Papers of particular interest, published within the period of review, have been highlighted as:

\* = important; \*\* = more important; \*\*\* = very important

- [1] Li, X.; Xu, Y.; Chen, Y.; Wang, C.; Jiang, J.; Dong, J.; Yan, H.; Du, X. Dual Enhanced Electrochemiluminescence of Aminated Au@SiO<sub>2</sub>/CdS Quantum Dot Superstructures: Electromagnetic Field Enhancement and Chemical Enhancement. *ACS Appl. Mater. Interfaces* **2019**, *11* (4), 4488–4499.
- [2] Liu, Y.; Chen, X.; Wang, M.; Ma, Q. A Visual Electrochemiluminescence Resonance Energy Transfer/Surface Plasmon Coupled Electrochemiluminescence Nanosensor for Shiga Toxin-Producing: Escherichia Coli Detection. *Green Chem.* **2018**, *20* (24), 5520–5527.
- [3] Bouffier, L.; Sojic, N. Introduction and Overview of Electrogenenerated Chemiluminescence. *RSC Detect. Sci.*



- [4] Valenti, G.; Rampazzo, E.; Bonacchi, S.; Khajvand, T.; Juris, R.; Montalti, M.; Marcaccio, M.; Paolucci, F.; Prodi, L. A Versatile Strategy for Tuning the Color of Electrochemiluminescence Using Silica Nanoparticles. *Chem. Commun.* **2012**, 48 (35), 4187–4189.
- [5] Rebecani, S.; Zanutt, A.; Santo, C. I.; Valenti, G.; Paolucci, F. A Guide Inside Electrochemiluminescent Microscopy Mechanisms for Analytical Performance Improvement. *Anal. Chem.* **2022**, 94, 336–348.
- [6] Du, F.; Chen, Y.; Meng, C.; Lou, B.; Zhang, W.; Xu, G. Recent Advances in Electrochemiluminescence Immunoassay Based on Multiple-Signal Strategy. *Curr. Opin. Electrochem.* **2021**, 28, 100725.
- [7] Ma, X.; Gao, W.; Du, F.; Yuan, F.; Yu, J.; Guan, Y.; Sojic, N.; Xu, G. Rational Design of Electrochemiluminescent Devices. *Acc. Chem. Res.* **2021**, 54 (14), 2936–2945.
- [8] Fiorani, A.; Valenti, G.; Iurlo, M.; Marcaccio, M.; Paolucci, F. Electrogenated Chemiluminescence: A Molecular Electrochemistry Point of View. *Curr. Opin. Electrochem.* **2018**, 8, 31–38.
- [9] Zhang, W.; Xiong, H.; Chen, M.; Zhang, X.; Wang, S. Surface-Enhanced Molecularly Imprinted Electrochemiluminescence Sensor Based on Ru@SiO<sub>2</sub> for Ultrasensitive Detection of Fumonisin B1. *Biosens. Bioelectron.* **2017**, 96, 55–61.
- [10] Zhang, Y.; Zhang, R.; Yang, X.; Qi, H.; Zhang, C. Recent Advances in Electrogenated Chemiluminescence Biosensing Methods for Pharmaceuticals. *J. Pharm. Anal.* **2019**, 9 (1), 9–19.
- [11] Choi, J. P.; Bard, A. J. Electrogenated Chemiluminescence (ECL) 79. Reductive-Oxidation ECL of Tris(2,2'-Bipyridine)Ruthenium(II) Using Hydrogen Peroxide as a Coreactant in PH 7.5 Phosphate Buffer Solution. *Anal. Chim. Acta* **2005**, 541 (1–2), 141–148.
- [12] Zhao, W.; Chen, H. Y.; Xu, J. J. Electrogenated Chemiluminescence Detection of Single Entities. *Chem. Sci.* **2021**, 12 (16), 5720–5736.
- [13] Yang, R.; Liu, Y.; Ye, H.; Qiu, B.; Lin, Z.; Guo, L. Surface Enhanced Electrochemiluminescence Immunoassay for Highly Sensitive Detection of Disease Biomarkers in Whole Blood. *Electroanalysis* **2016**, 28 (8), 1783–1786.
- [14] Nikolaou, P.; Sciuto, E. L.; Zanutt, A.; Petralia, S.; Valenti, G.; Paolucci, F.; Prodi, L.; Conoci, S. Ultrasensitive PCR-Free Detection of Whole Virus Genome by Electrochemiluminescence. *Biosens. Bioelectron.* **2022**, 209, 114165.
- [15] Jie, G.; Zhou, Q.; Jie, G. Graphene Quantum Dots-Based Electrochemiluminescence Detection of DNA Using Multiple Cycling Amplification Strategy. *Talanta* **2019**, 194, 658–663.
- [16] Jie, G.; Lu, Z.; Zhao, Y.; Wang, X. Quantum Dots Bilayers/Au@Ag-Based Electrochemiluminescence Resonance Energy Transfer for Detection of Thrombin by Autocatalytic Multiple Amplification Strategy. *Sensors Actuators, B Chem.* **2017**, 240, 857–862.
- [17] Zhou, L.; Huang, J.; Yu, B.; Liu, Y.; You, T. A Novel Electrochemiluminescence Immunosensor for the Analysis of HIV-1 P24 Antigen Based on P-RGO@Au@Ru-SiO<sub>2</sub> Composite. *ACS Appl. Mater. Interfaces* **2015**, 7 (44), 24438–24445.
- [18] Wang, D.; Li, Y.; Lin, Z.; Qiu, B.; Guo, L. Surface-Enhanced Electrochemiluminescence of Ru@SiO<sub>2</sub> for Ultrasensitive Detection of Carcinoembryonic Antigen. *Anal. Chem.* **2015**, 87 (12), 5966–5972.
- [19] Luo, L.; Ma, S.; Li, L.; Liu, X.; Zhang, J.; Li, X.; Liu, D.; You, T. Monitoring Zearalenone in Corn Flour Utilizing Novel Self-Enhanced Electrochemiluminescence Aptasensor Based on NGQDs-NH<sub>2</sub>-Ru@SiO<sub>2</sub> Luminophore. *Food Chem.* **2019**, 292, 98–105.
- [20] Li, L.; Chen, B.; Luo, L.; Liu, X.; Bi, X.; You, T. Sensitive and Selective Detection of Hg<sup>2+</sup> in Tap and Canal Water via Self-Enhanced ECL Aptasensor Based on NH<sub>2</sub>-Ru@SiO<sub>2</sub>-NGQDs. *Talanta* **2021**, 222, 1–8.

- [21] Cao, N.; Zeng, P.; Zhao, F.; Zeng, B. Au@SiO<sub>2</sub>@RuDS Nanocomposite Based Plasmon-Enhanced Electrochemiluminescence Sensor for the Highly Sensitive Detection of Glutathione. *Talanta* **2019**, *204*, 402–408.
- [22] Wang, J.; Zhao, W. W.; Zhou, H.; Xu, J. J.; Chen, H. Y. Amplified Electrochemiluminescence Detection of DNA-Binding Protein Based on the Synergy Effect of Electron and Energy Transfer between CdS Nanocrystals and Gold Nanoparticles. *Biosens. Bioelectron.* **2013**, *41* (1), 615–620.
- [23] Han, T.; Li, X.; Li, Y.; Cao, W.; Wu, D.; Du, B.; Wei, Q. Gold Nanoparticles Enhanced Electrochemiluminescence of Graphite-like Carbon Nitride for the Detection of Nuclear Matrix Protein 22. *Sensors Actuators, B Chem.* **2014**, *205*, 176–183.
- [24] Wang, J.; Shan, Y.; Zhao, W. W.; Xu, J. J.; Chen, H. Y. Gold Nanoparticle Enhanced Electrochemiluminescence of CdS Thin Films for Ultrasensitive Thrombin Detection. *Anal. Chem.* **2011**, *83* (11), 4004–4011.
- [25] Wu, M.; He, L.; Xu, J.; Chen, H. RuSi@Ru(Bpy)<sub>3</sub><sup>2+</sup>/Au@Ag<sub>2</sub>S Nanoparticles Electrochemiluminescence Resonance Energy Transfer System for Sensitive DNA Detection. *Anal. Chem.* **2014**, *86*, 4559–4565.
- [26] Zanut, A.; Palomba, F.; Rossi Scota, M.; Rebecani, S.; Marcaccio, M.; Genovese, D.; Rampazzo, E.; Valenti, G.; Paolucci, F.; Prodi, L. Dye-Doped Silica Nanoparticles for Enhanced ECL-Based Immunoassay Analytical Performance. *Angew. Chemie - Int. Ed.* **2020**, *59* (49), 21858–21863.
- [27] Wang, D.; Zhou, J.; Guo, L.; Qiu, B.; Lin, Z. A Surface-Enhanced Electrochemiluminescence Sensor Based on Au-SiO<sub>2</sub> Core-Shell Nanocomposites Doped with Ru(Bpy)<sub>3</sub><sup>2+</sup> for the Ultrasensitive Detection of Prostate-Specific Antigen in Human Serum. *Analyst* **2020**, *145* (1), 132–138. The LSPR produced by the Au of Au@SiO<sub>2</sub>-Ru greatly improved the ECL sensitivity to detect PSA and the performance of ECL depends on the size and shape of the nanostructure and distance of Au core to Ru(bpy)<sub>3</sub><sup>2+</sup>.  
\*\*\*
- [28] Ding, L.; Xu, S.; Huang, D.; Chen, L.; Kannan, P.; Guo, L.; Lin, Z. Surface-Enhanced Electrochemiluminescence Combined with Resonance Energy Transfer for Sensitive Carcinoembryonic Antigen Detection in Exhaled Breath Condensates. *Analyst* **2020**, *145* (20), 6524–6531. A sensitive dual signal amplification strategy was developed based on surface-enhanced electrochemiluminescence (SEECLE) combined with resonance energy transfer (RET) to detect CEA. The graphite-like carbon nitride nanosheets (g-C<sub>3</sub>N<sub>4</sub> NS) was used as an energy donor, and Ru(bpy)<sub>3</sub><sup>2+</sup> as an acceptor to amplify ECL signal. Moreover, the LSPR of gold nanoparticles (Au NPs) has contributed to enhance the ECL signal of Ru(bpy)<sub>3</sub><sup>2+</sup>.  
\*\*\*
- [29] Kitte, S. A.; Tafese, T.; Xu, C.; Saqib, M.; Li, H.; Jin, Y. Plasmon-Enhanced Quantum Dots Electrochemiluminescence Aptasensor for Selective and Sensitive Detection of Cardiac Troponin I. *Talanta* **2021**, *221*, 121674. The ECL signal of CdS QDs showed about 5-fold increment as compared to that of without AuNPs and was able to detect ultralow level of cardiac troponin I (cTnI)  
\*
- [30] Dutta, P.; Han, D.; Goudeau, B.; Jiang, D.; Fang, D.; Sojic, N. Reactivity Mapping of Luminescence in Space: Insights into Heterogeneous Electrochemiluminescence Bioassays. *Biosens. Bioelectron.* **2020**, *165*, 112372.
- [31] Ma, C.; Cao, Y.; Gou, X.; Zhu, J. J. Recent Progress in Electrochemiluminescence Sensing and Imaging. *Anal. Chem.* **2020**, *92*, 431–454.
- [32] Jones, A.; Dhanapala, L.; Kankanamage, R. N. T.; Kumar, C. V.; Rusling, J. F. Multiplexed Immunosensors and Immunoarrays. *Anal. Chem.* **2020**, *92* (1), 345–362.
- [33] Kerr, E.; Hayne, D. J.; Soulsby, L. C.; Bawden, J. C.; Blom, S. J.; Doeven, E. H.; Henderson, L. C.; Hogan, C. F.; Francis, P. S. A Redox-Mediator Pathway for Enhanced Multi-Colour Electrochemiluminescence in Aqueous Solution. *Chem. Sci.* **2022**, *13*, 469–477.
- [34] Zanut, A.; Fiorani, A.; Canola, S.; Saito, T.; Ziebart, N.; Rapino, S.; Rebecani, S.; Barbon, A.; Irie, T.; Josel, H. P.; Negri, F.; Marcaccio, M.; Windfuhr, M.; Imai, K.; Valenti, G.; Paolucci, F. Insights into the Mechanism of Coreactant Electrochemiluminescence Facilitating Enhanced Bioanalytical Performance.

*Nat. Commun.* **2020**, *11* (1), 1–9.

- [35] Yuan, Y.; Han, S.; Hu, L.; Parveen, S.; Xu, G. Coreactants of Tris(2,2'-Bipyridyl)Ruthenium(II) Electrogenerated Chemiluminescence. *Electrochim. Acta* **2012**, *82*, 484–492.
- [36] Irkham; Fiorani, A.; Valenti, G.; Kamoshida, N.; Paolucci, F.; Einaga, Y. Electrogenerated Chemiluminescence by in Situ Production of Coreactant Hydrogen Peroxide in Carbonate Aqueous Solution at a Boron-Doped Diamond Electrode. *J. Am. Chem. Soc.* **2020**, *142* (3), 1518–1525.
- [37] Kesarkar, S.; Valente, S.; Zanut, A.; Palomba, F.; Fiorani, A.; Marcaccio, M.; Rampazzo, E.; Valenti, G.; Paolucci, F.; Prodi, L. Neutral Dye-Doped Silica Nanoparticles for Electrogenerated Chemiluminescence Signal Amplification. *J. Phys. Chem. C* **2019**, *123* (9), 5686–5691.
- [38] Carrara, S.; Arcudi, F.; Prato, M.; De Cola, L. Amine-Rich Nitrogen-Doped Carbon Nanodots as a Platform for Self-Enhancing Electrochemiluminescence. *Angew. Chemie - Int. Ed.* **2017**, *56* (17), 4757–4761.
- [39] Wang, D.; Guo, L.; Huang, R.; Qiu, B.; Lin, Z.; Chen, G. Surface Enhanced Electrochemiluminescence for Ultrasensitive Detection of Hg<sup>2+</sup>. *Electrochim. Acta* **2014**, *150*, 123–128.
- [40] Kesarkar, S.; Rampazzo, E.; Zanut, A.; Palomba, F.; Marcaccio, M.; Valenti, G.; Prodi, L.; Paolucci, F. Dye-Doped Nanomaterials: Strategic Design and Role in Electrochemiluminescence. *Curr. Opin. Electrochem.* **2018**, *7*, 130–137.
- [41] Rebecani, S.; Wetzl, C.; Zamolo, V. A.; Criado, A.; Valenti, G.; Paolucci, F.; Prato, M. Electrochemiluminescent Immunoassay Enhancement Driven by Carbon Nanotubes. *Chem. Commun.* **2021**, *57* (76), 9672–9675.
- [42] Zhang, S.; Liu, Y. Recent Progress of Novel Electrochemiluminescence Nanoprobes and Their Analytical Applications. *Front. Chem.* **2021**, *8*, 1–7. The performance and applications of ECL nanoprobes are highly associated with structure, type, size and design of the nanostructures.
- [43] Adsetts, J. R.; Ding, Z. Film Electrochemiluminescence Controlled by Interfacial Reactions Along with Aggregation-, Matrix-Coordination-, and Crystallization-Induced Emissions. *Chempluschem* **2021**, *86* (1), 155–165.
- [44] Arcudi, F.; Đorđević, L.; Rebecani, S.; Cacioppo, M.; Zanut, A.; Valenti, G.; Paolucci, F.; Prato, M. Lighting up the Electrochemiluminescence of Carbon Dots through Pre- and Post-Synthetic Design. *Adv. Sci.* **2021**, *8* (13), 1–9.
- [45] Liu, Y.; Zhang, H.; Li, B.; Liu, J.; Jiang, D.; Liu, B.; Sojic, N. Single Biomolecule Imaging by Electrochemiluminescence. *J. Am. Chem. Soc.* **2021**, *143* (43), 17910–17914.
- [46] Gai, Q. Q.; Wang, D. M.; Huang, R. F.; Liang, X. X.; Wu, H. L.; Tao, X. Y. Distance-Dependent Quenching and Enhancing of Electrochemiluminescence from Tris(2, 2'-Bipyridine) Ruthenium (II)/Tripropylamine System by Gold Nanoparticles and Its Sensing Applications. *Biosens. Bioelectron.* **2018**, *118*, 80–87.
- [47] Yin, X. B.; Qi, B.; Sun, X.; Yang, X.; Wang, E. 4-(Dimethylamino)Butyric Acid Labeling for Electrochemiluminescence Detection of Biological Substances by Increasing Sensitivity with Gold Nanoparticle Amplification. *Anal. Chem.* **2005**, *77* (11), 3525–3530.
- [48] Wang, X.; Wang, Y.; Jiang, M.; Shan, Y.; Jin, X.; Gong, M.; Wang, X. Functional Electrospun Nanofibers-Based Electrochemiluminescence Immunosensor for Detection of the TSP 53 Using RuAg/SiO<sub>2</sub> NPs as Signal Enhancers. *Anal. Biochem.* **2018**, *548*, 15–22.
- [49] Huang, R.; Wei, M. Y.; Guo, L. H. Enhanced Electrogenerated Chemiluminescence of Ru(Bpy)<sub>3</sub><sup>2+</sup>/Tripropylamine System on Indium Tin Oxide Nanoparticle Modified Transparent Electrode. *J. Electroanal. Chem.* **2011**, *656* (1–2), 136–139.
- [50] Lakowicz, J. R. Radiative Decay Engineering 5: Metal-Enhanced Fluorescence and Plasmon Emission. *Anal. Biochem.* **2005**, *337* (2), 171–194.

- [51] Zhang, J.; Gryczynski, Z.; Lakowicz, J. R. First Observation of Surface Plasmon-Coupled Electrochemiluminescence. *Chem. Phys. Lett.* **2004**, 393 (4–6), 483–487.
- [52] Dinel, M. P.; Tartaglia, S.; Wallace, G. Q.; Boudreau, D.; Masson, J. F.; Polo, F. The Fundamentals of Real-Time Surface Plasmon Resonance/ Electrogenerated Chemiluminescence. *Angew. Chemie - Int. Ed.* **2019**, 58, 18202–18206.
- [53] Wang, D.; Guo, L.; Huang, R.; Qiu, B.; Lin, Z.; Chen, G. Surface Enhanced Electrochemiluminescence of Ru(Bpy)<sub>3</sub><sup>2+</sup>. *Sci. Rep.* **2015**, 5, 1–7.
- [54] Feng, X.; Han, T.; Xiong, Y.; Wang, S.; Dai, T.; Chen, J.; Zhang, X.; Wang, G. Plasmon-Enhanced Electrochemiluminescence of Silver Nanoclusters for MicroRNA Detection. *ACS Sensors* **2019**, 4 (6), 1633–1640.
- [55] Miao, Y. B.; Ren, H. X.; Gan, N.; Zhou, Y.; Cao, Y.; Li, T.; Chen, Y. A Triple-Amplification SPR Electrochemiluminescence Assay for Chloramphenicol Based on Polymer Enzyme-Linked Nanotracers and Exonuclease-Assisted Target Recycling. *Biosens. Bioelectron.* **2016**, 86, 477–483.
- [56] Han, D.; Li, X.; Bian, X.; Wang, J.; Kong, L.; Ding, S.; Yan, Y. Localized Surface Plasmon-Enhanced Electrochemiluminescence Biosensor for Rapid, Label-Free, and Single-Step Detection of Broad-Spectrum Bacteria Using Urchin-like Au and Ag Nanoparticles. *Sensors Actuators B Chem.* **2021**, 355, 131120. LSPR enhanced ECL biosensor was designed from urchin-like Au and Ag nanoparticles for rapid, one-step, and label-free detection of broad-spectrum bacteria.
- [57] Ma, Q.; Zhang, Q.; Tian, Y.; Liang, Z.; Wang, Z.; Xu, S. DNA-Mediated Au-Au Dimer-Based Surface Plasmon Coupling Electrochemiluminescence Sensor for BRCA1 Gene Detection. *Anal. Chem.* **2021**, 93 (6), 3308–3314.
- [58] Li, J.; Shan, X.; Jiang, D.; Wang, W.; Xu, F.; Chen, Z. Au Nanoparticle Plasmon-Enhanced Electrochemiluminescence Aptasensor Based on the 1D/2D PTCA/CoP for Diclofenac Assay. *Microchim. Acta* **2021**, 188 (7).
- [59] Zhang, J. ran; Kan, Y. shi; Gu, L. ling; Wang, C. yin; Zhang, Y. Graphite Carbon Nitride and Its Composites for Medicine and Health Applications. *Chem. - An Asian J.* **2021**, 16 (15), 2003–2013.
- [60] Kumarswamy, R.; Volkmann, I.; Thum, T. Regulation and Function of MiRNA-21 in Health and Disease. *RNA Biol.* **2011**, 8 (5), 706–713.
- [61] Li, M. X.; Zhang, N.; Zhao, W.; Luo, X. L.; Chen, H. Y.; Xu, J. J. Ultrasensitive Detection of MicroRNA-21 Based on Plasmon-Coupling-Induced Electrochemiluminescence Enhancement. *Electrochem. commun.* **2018**, 94, 36–40.
- [62] Li, C.; Wang, S.; Li, H.; Saqib, M.; Xu, C.; Jin, Y. Nanoengineered Metasurface Immunosensor with over 1000-Fold Electrochemiluminescence Enhancement for Ultra-Sensitive Bioassay. *iScience* **2019**, 17, 267–276.
- [63] Voci S., Duwald R., Grass S., J. Hayne D., Bouffier L., S. Francis P., L. J. and S. N. Self-Enhanced Multicolor Electrochemiluminescence by Competitive Electron-Transfer Processes. *Chem. Sci.* **2020**, 11, 4508–4515.
- [64] Genovese, D.; Rampazzo, E.; Bonacchi, S.; Montalti, M.; Zaccheroni, N.; Prodi, L. Energy Transfer Processes in Dye-Doped Nanostructures Yield Cooperative and Versatile Fluorescent Probes. *Nanoscale* **2014**, 6 (6), 3022–3036.
- [65] Wang, H.; Peng, L.; Chai, Y.; Yuan, R. High-Sensitive Electrochemiluminescence C-Peptide Biosensor via the Double Quenching of Dopamine to the Novel Ru(II)-Organic Complex with Dual Intramolecular Self-Catalysis. *Anal. Chem.* **2017**, 89 (20), 11076–11082.
- [66] Feng, Q. M.; Shen, Y. Z.; Li, M. X.; Zhang, Z. L.; Zhao, W.; Xu, J. J.; Chen, H. Y. Dual-Wavelength Electrochemiluminescence Ratiometry Based on Resonance Energy Transfer between Au Nanoparticles

- Functionalized g-C<sub>3</sub>N<sub>4</sub> Nanosheet and Ru(Bpy)<sub>3</sub><sup>2+</sup> for MicroRNA Detection. *Anal. Chem.* **2016**, 88 (1), 937–944.
- [67] Liu, J. L.; Zhao, M.; Zhuo, Y.; Chai, Y. Q.; Yuan, R. Highly Efficient Intramolecular Electrochemiluminescence Energy Transfer for Ultrasensitive Bioanalysis of Aflatoxin M1. *Chem. - A Eur. J.* **2017**, 23 (8), 1853–1859.
- [68] Chen, M. M.; Wang, Y.; Cheng, S. B.; Wen, W.; Zhang, X.; Wang, S.; Huang, W. H. Construction of Highly Efficient Resonance Energy Transfer Platform Inside a Nanosphere for Ultrasensitive Electrochemiluminescence Detection. *Anal. Chem.* **2018**, 90 (8), 5075–5081.
- [69] Li, Z.; Lin, Z.; Wu, X.; Chen, H.; Chai, Y.; Yuan, R. Highly Efficient Electrochemiluminescence Resonance Energy Transfer System in One Nanostructure: Its Application for Ultrasensitive Detection of MicroRNA in Cancer Cells. *Anal. Chem.* **2017**, 89 (11), 6029–6035.
- [70] Shan, Y.; Xu, J. J.; Chen, H. Y. Distance-Dependent Quenching and Enhancing of Electrochemiluminescence from a CdS:Mn Nanocrystal Film by Au Nanoparticles for Highly Sensitive Detection of DNA. *Chem. Commun.* **2009**, 8, 905–907.
- [71] Wu, M. S.; Shi, H. W.; Xu, J. J.; Chen, H. Y. CdS Quantum Dots/Ru(Bpy)<sub>3</sub><sup>2+</sup> Electrochemiluminescence Resonance Energy Transfer System for Sensitive Cytosensing. *Chem. Commun.* **2011**, 47 (27), 7752–7754.
- [72] Dong, Y.; Gao, T.; Zhou, Y.; Zhu, J. Electrogenated Chemiluminescence Resonance Energy Transfer between Luminol and CdSe@ZnS Quantum Dots and Its Sensing Application in the Determination of Thrombin. *Anal. Chem.* **2014**, 86, 11373–11379.
- [73] Zhang, S.; Zheng, H.; Chen, Y.; Yi, H.; Dai, H.; Hong, Z.; Lin, Y. Electrochemiluminescence Resonance Energy Transfer between Ru(Bpy)<sub>3</sub><sup>2+</sup> and CdZnSe@ZnSe Quantum Dots for Ovarian Cancer Biomarker Detection. *ACS Appl. Nano Mater.* **2019**, 2 (11), 7061–7066. An enhanced ECL biosensor based on RET from Ru(bpy)<sub>3</sub><sup>2+</sup> (loaded in TiO<sub>2</sub> MOFs) to CdZnSe@ZnSe quantum dots was designed and ultralow level of ovarian cancer biomarker was detected.
- [74] Xie, N.; Liu, S.; Yang, X.; He, X.; Huang, J.; Wang, K. DNA Tetrahedron Nanostructures for Biological Applications: Biosensors and Drug Delivery. *Analyst* **2017**, 142 (18), 3322–3332.
- [75] Lu, H. J.; Pan, J. Bin; Wang, Y. Z.; Ji, S. Y.; Zhao, W.; Luo, X. L.; Xu, J. J.; Chen, H. Y. Electrochemiluminescence Energy Resonance Transfer System between RuSi Nanoparticles and Hollow Au Nanocages for Nucleic Acid Detection. *Anal. Chem.* **2018**, 90 (17), 10434–10441.